Supporting Information

Sensitive detection of protein biomarkers using silver nanoparticles enhanced immunofluorescence assay

Li-Jun Zhao[1†], Ru-Jia Yu[1†], Wei Ma[1], Huan-Xing Han[2], He Tian[1], Ruo-Can Qian[1]*, Yi-Tao Long[1]*

1. Key Laboratory for Advanced Materials and Department of Chemistry, School of Chemistry and Molecular Engineering, East China University of Science and Technology, P.R. China.

2. Translational Medicine Center, Changzheng Hospital, the Second Military Medical University, P.R. China.

Corresponding authors: Y.T.L (ytlong@ecust.edu.cn) or R.C.Q (ruocanqianecust@163.com)

Contents

1. The synthesis and characterization of Ag^+ fluorescence probe (Ag^+-FP) S2

2. The characterization of silver nanoparticles (AgNPs) S3

4. Fluorescence response of different size AgNPs for AFP S6

5. Time dependent fluorescence intensity change of 60 nm AgNPs S7

7. Determination of detection limit S8

8. The comparison of fluorescence immunoassay with different strategies S8

9. The ^{1}H NMR, ^{13}C NMR and MS characterization of target compounds and intermediates S10

10. References S13

1. The synthesis and characterization of Ag^+ fluorescence probe (Ag^+-FP)

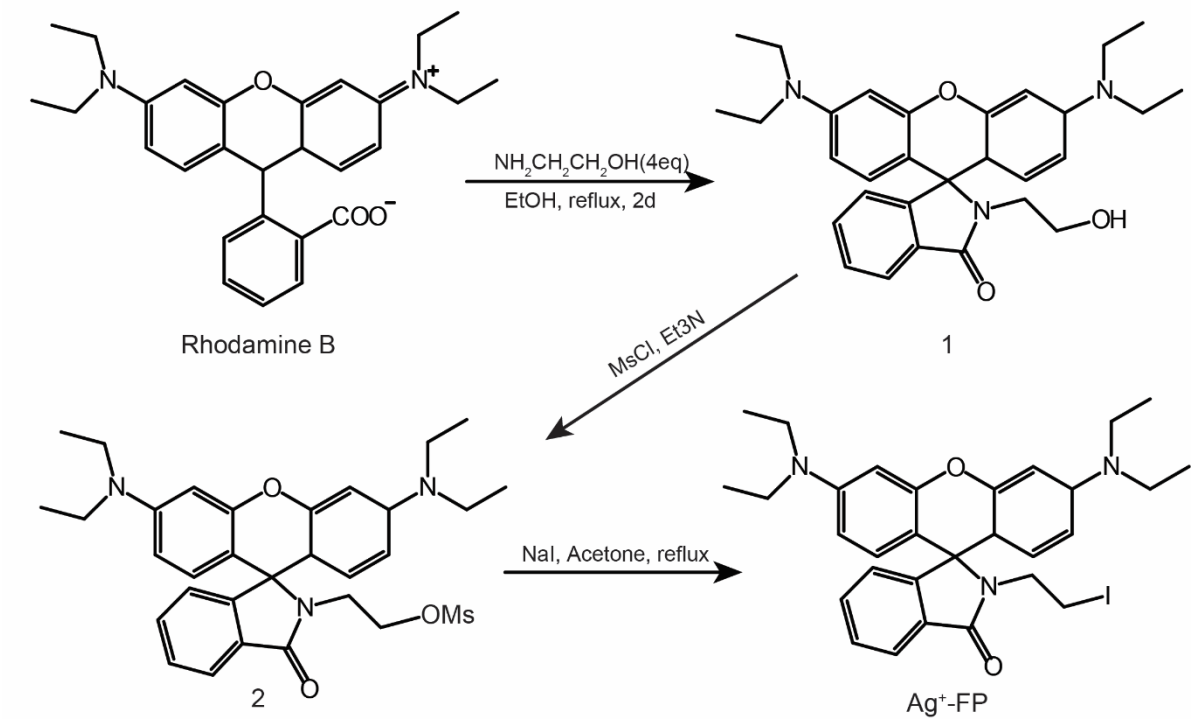

Figure S1. The synthesis of Ag^+ fluorescence probe (Ag^+-FP).

Synthesis of 3', 6'-bis (diethylamino)-2-(2-hydroxyethyl)-3', 9'-dihydrospiro [isoindoline-1, 9'-xanthen]-3-one (1). Typically, 2-aminoethanol (252 μL, 4.16 mmol) was added to a solution of Rhodamine B (0.500 g, 1.04 mmol) in ethanol (40 mL), and the resulting mixture was heated at 120 °C for 2 days. The reaction mixture was cooled to room temperature and the solvent was evaporated under vacuo. The residue obtained was dissolved in EtOAc (30 mL) and successively washed with water (20 mL) and brine (10 mL), dried over Na_2SO_4 and evaporated under vacuo. Finally, the solid obtained was purified by silica gel chromatography (10 % MeOH in CH_2Cl_2) to get compound 1 as a white solid. ^{1}H NMR (400 MHz, $CDCl_3$) δ = 7.95 – 7.82 (m, 1H), 7.44 (dt, J = 7.3, 3.7 Hz, 2H), 7.15 – 6.98 (m, 1H), 6.49 (d, J = 8.8 Hz, 2H), 6.38 (d, J = 2.5 Hz, 2H), 6.29 (dd, J = 8.9, 2.6 Hz, 2H), 4.21 (t, J = 5.5 Hz, 1H), 3.47 (dd, J = 9.6, 4.9 Hz, 2H), 3.39 – 3.22 (m, 10H), 1.16 (t, J = 7.1 Hz, 12H). ^{13}C NMR (101 MHz, $CDCl_3$) δ = 170.10, 153.91, 153.27, 148.88, 132.71, 130.43, 128.51, 128.15, 123.81, 122.90, 108.22, 104.75, 97.77, 65.88, 62.66, 44.63, 44.37, 12.60 (s). HRMS (ESI): m/z calcd for $C_{30}H_{36}O_3N_3$ [$(M+H^+)$] 486.2757; Found 486.2747.

Synthesis of 3', 6'-bis(diethylamino)-2-(2-iodoethyl)-3', 9a'-dihydrospiro[isoindoline-1, 9'-xanthen]-3-one (Ag^+-FP). A 100 mL round-bottomed flask were placed compound **1** (0.200 g, 0.41 mmol), triethyl-amine (0.630 g, 0.62 mmol) and dichloromethane (30 mL) under argon atmosphere. The mixture was cooled in an ice bath and then 38 μL of methanesulfonyl chloride was added dropwise. The reaction mixture was stirred at room temperature for overnight. It was washed successively with water (2×10 mL) and brine (10 mL). The organic layer was dried over Na_2SO_4 and evaporated under vacuo. The residue **2** obtained was directly used for next step reaction without further purification. The above mesylate were added 20 mL of dry acetone and 0.076 g (0.5 mmol) anhydrous sodium iodide under inert atmosphere, and the reaction mixture was refluxed for 12 h. Then it was cooled down to room temperature and the solvent was removed under vacuo. The residue obtained was dissolved in dichloromethane and washed with 10 % aqueous sodium thiosulfate solution (10 mL) and brine (10 mL), respectively. The organic layer was dried over Na_2SO_4 and evaporated under vacuo to get a white solid. ^{1}H NMR (400 MHz, $CDCl_3$) δ = 7.83 (dd, J = 5.7, 2.7 Hz, 1H), 7.44 – 7.29 (m, 2H), 6.98 (dd, J = 5.7, 2.6 Hz, 1H), 6.37 (s, 1H), 6.35 (s, 1H), 6.31 (d, J = 2.4 Hz, 2H), 6.19 (dd, J = 8.9, 2.5 Hz, 2H), 3.54 – 3.39 (m, 2H), 3.27 (q, J = 7.1 Hz, 8H), 2.82 – 2.66 (m, 2H), 1.10 (t, J = 7.0 Hz, 12H). ^{13}C NMR (101 MHz, $CDCl_3$) δ = 165.84, 151.58, 151.21, 146.91, 130.70, 128.60, 126.73, 126.12, 121.82, 120.97, 106.18, 103.23, 95.82, 62.70, 42.38, 41.09, 10.63. HRMS: (FAB) m/z calcd for $C_{30}H_{35}O_2N_3I$ [$(M+H^+)$] 596.1776; found 596.1766.

2. The characterization of silver nanoparticles (AgNPs)

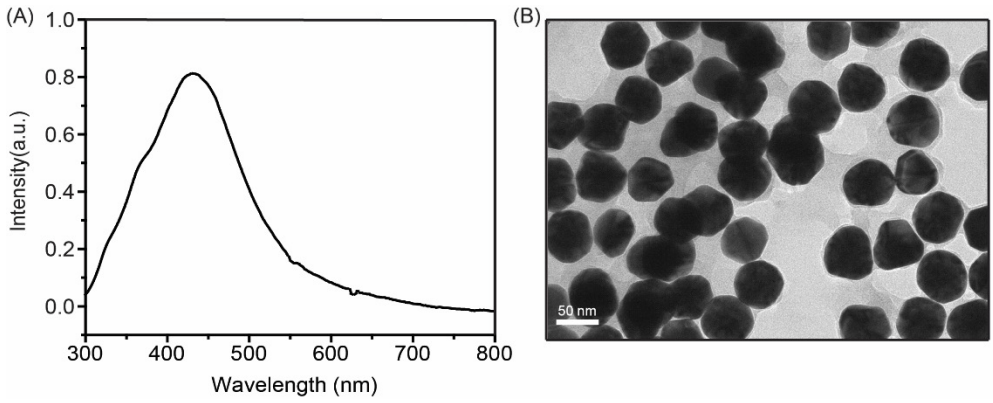

Figure S2. UV-Vis spectrum (a) and TEM image (b) of the synthesized silver nanoparticles with a diameter about 60 nm.

3. The characterization of immuno-complexes Ab1-MBs@AG@Ab2-AgNPs

The conjugation of labeled antibody Ab2 on the surface of silver nanoparticles AgNPs was evaluated by immunofluorescence experiments. Typically, 50 μL of Ab2-AgNPs blocked with BSA was first transferred into a 0.5-mL Eppendorf tube, and then 100 μL of 10^{-6} g mL^{-1} Cy5-labeled second antibody solution were added, the mixture was incubated for 30 min at 37 °C with gentle mixing in a TS-100 ThermoShaker. The solution was repeatedly centrifuged under optimized conditions to get rid of the excess Cy5-labelled second antibody. The obtained Ab2-AgNPs modified with Cy5-labelled second antibody was re-dispersed into 100μL PBS (50 mM, pH 7.4) and its fluorescence was measured by fluorescence microscope. A similar experiment was also performed using BSA blocked AgNPs without Ab2 on the surface of AgNPs. As shown in Figure S3, for BSA blocked AgNPs, almost no fluorescence emission was observed at 664 nm. While the fluorescence intensity obviously enhanced for Ab2-AgNPs blocked with BSA. These results demonstrate the successful binding of Ab2 on the surface of AgNPs.

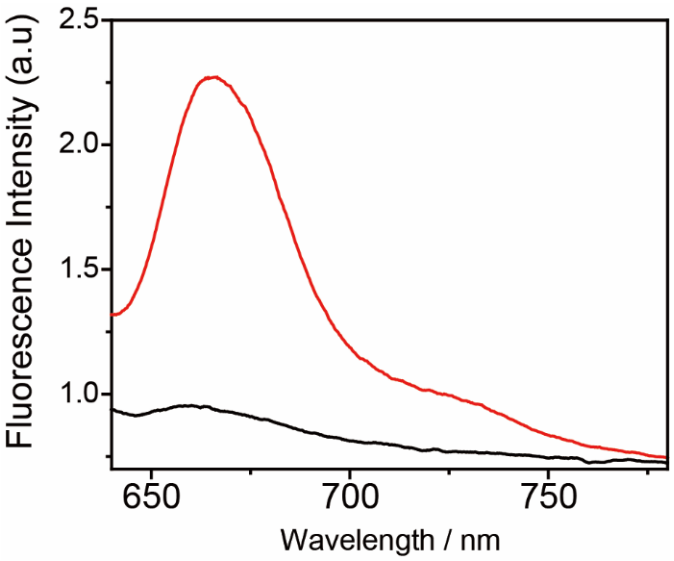

Figure S3. Fluorescence spectra of BSA blocked AgNPs (black line) and Ab2-AgNPs (red line) after incubating with Cy5 labelled second antibodies solution (10^{-6} g mL^{-1}) (ex: 646 nm; em: 664 nm).

Immunofluorescence experiments were also used to evaluate the conjugation of antibody Ab1 on the surface of MBs. Typically, 50 μL of Ab1-MBs blocked with BSA was first transferred into a 0.5-mL Eppendorf tube, and 100 μL of 10^{-6} g mL^{-1} Cy5-labelled second antibody solution were added, the mixture

was incubated for 30 min at 37 °C with gentle mixing in a TS-100 ThermoShaker. After washing three times with phosphate buffer solution (50 mm, pH 7.4) including 0.05 % (v/v) Tween 20 (PBST), the Ab1-MBs was re-dispersed into 100 μL PBS (50 mM, pH 7.4) and its fluorescence was measured by fluorescence microscope. A similar experiment was also performed using BSA blocked MBs without Ab1. As shown in Figure S4, for BSA blocked MBs, almost no fluorescence emission was observed at 664 nm. While the fluorescence intensity obviously enhanced for Ab1-MBs blocked with BSA. These results demonstrate the successful binding of Ab1 on the surface of MBs.

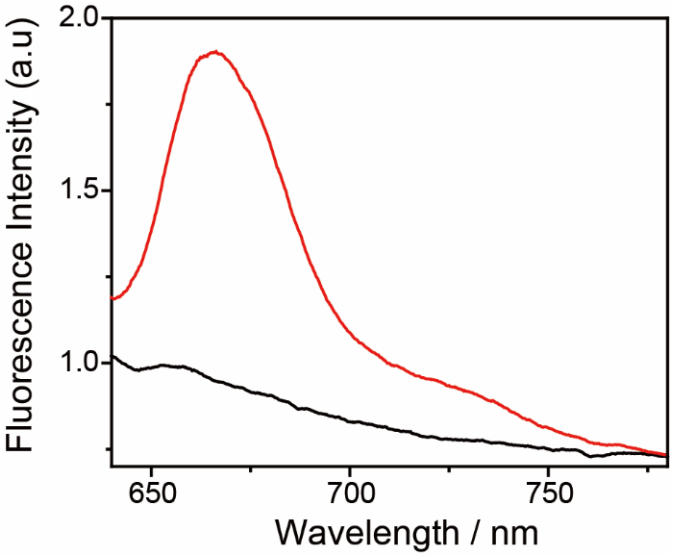

Figure S4. Fluorescence spectra of BSA blocked MBs (black line) and Ab1-MBs (red line) after incubating with Cy5 labelled second antibodies solution (10^{-6} g mL^{-1}) (ex: 646 nm; em: 664 nm).

In addition, in order to characterize the formation of immuno-complexes Ab1-MBs@AG@Ab2-AgNPs, the TEM images of single magnetic beads (analytes captured) Ab1-MBs@AG before and after binding Ab2-AgNPs have been demonstrated. As shown in Figure S5, there was no AgNPs could be observed for Ab1-MBs@AG before bound with Ab2-AgNPs (Figure S5A). However, it was clearly seen that AgNPs were combined on the surface of MBs (Figure S5B), which demonstrated an effectively binding of Ab1-MBs@AG with Ab2-AgNPs.

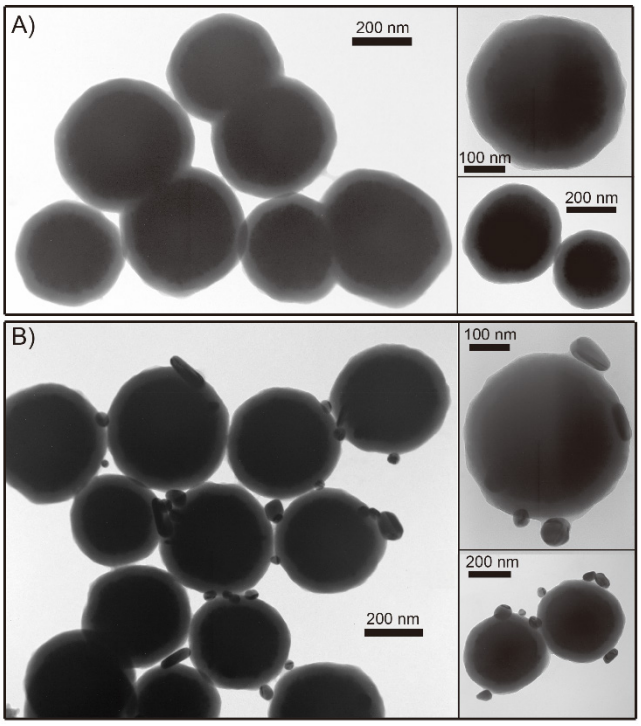

Figure S5. The TEM images of single magnetic beads (analytes captured) Ab1-MBs@AG before (A) and after (B) binding Ab2-AgNPs.

4. Fluorescence response of different size AgNPs for AFP

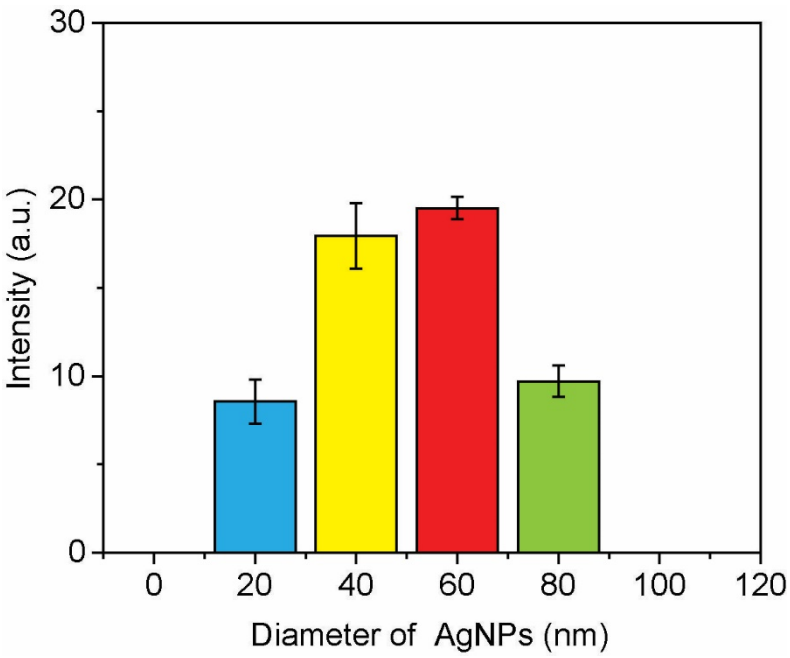

Figure S6. Variation in the analytical signal with different sizes of the silver nanoparticles at a concentration of 10 ng / mL AFP.

5. Time dependent fluorescence intensity change of 60 nm AgNPs

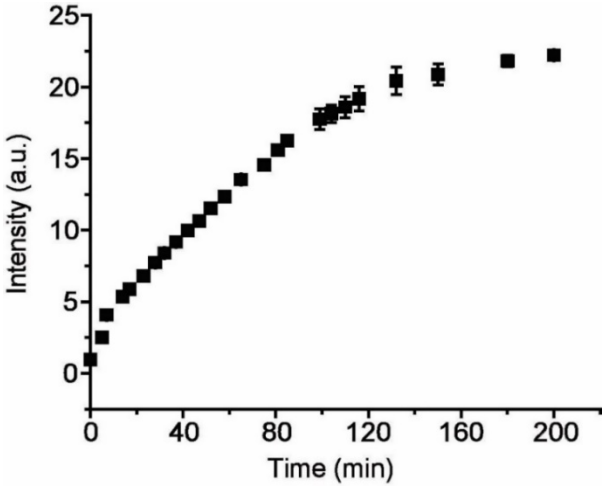

Figure S7. Time dependent fluorescence intensity of Ag^{+}-FP solution containing 50 mM H_2O_2 in the presence of 10 pM AgNPs (60 nm) (ex: 540 nm; em: 585 nm).

6. The amount of antibody adsorbed to silver nanoparticles

The concentration of antibody was optimized to better combine with silver nanoparticles in AFP detection. An AFP concentration of 10 ng mL^{-1} was used to the experiment. As depicted in Figure S5, the concentration of antibody should be five times higher than that of AgNPs. Therefore, in the following experiment, a concentration of antibody that of ten times AgNPs was used to do the combination.

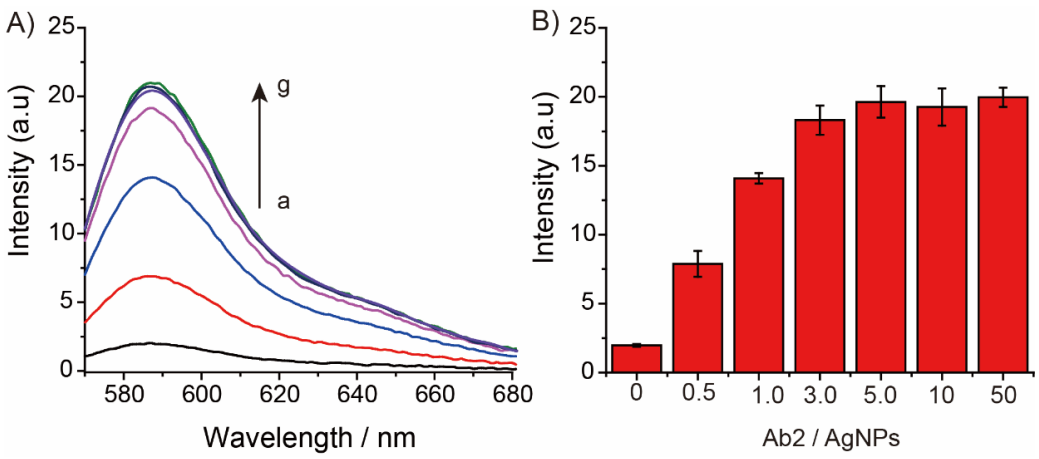

Figure S8. A) Fluorescence spectra of the immuno-system with a different concentrations antibody (eq. AgNPs) modified AgNPs for AFP detection (from a to g: 0, 0.5, 1.0, 3.0, 5.0, 10, 50). The AFP concentration was 10 ng mL^{-1}. B) The fluorescence intensity (585 nm) versus the concentrations antibody (eq.AgNPs).

7. Determination of detection limit

The limit of detection (LOD) of Ag^+-FP for Ag^+ and the detection system for antigen were determined from the following equation:

$$LOD = 3 \times \sigma / k \quad \text{(S1)}$$

Where σ is the standard deviation of the blank measurement; k is the slope between the fluorescence intensity versus analyte concentration.

From the graph of Ag^+-FP for Ag^+ detection, we could get $k_{Ag+} = 5.446$ from equation (S2), and $\sigma_{Ag+} = 0.102$ from blank measurement. Thus the LOD of Ag^+ could be calculated to be 0.06 μM, i.e. the Ag^+-FP can detect Ag^+ in this minimum concentration by fluorescence techniques. The theoretical LOD of probe Ag^+-FP for target antigens can be calculated to be 0.06 pM based on 60 nm AgNPs.[S1-S2]

$$Y = 5.446X + 1.146 \quad \text{(S2)}$$

From the graph of AFP detection, we could get $k_{AFP} = 1.449$ from equation (S3), and $\sigma_{AFP} = 0.0358$ from blank measurement. Thus the LOD of AFP could be calculated to be 70 $pg \cdot mL^{-1}$.

$$Y = 1.449X + 5.566 \quad \text{(S3)}$$

From the graph of CRP detection, we could get $k_{CRP} = 1.261$ from equation (S4), and $\sigma_{CRP} = 0.0128$ from blank measurement. Thus the LOD of CRP could be calculated to be 30 $pg \cdot mL^{-1}$.

$$Y = 1.261X + 4.656 \quad \text{(S4)}$$

8. The comparison of fluorescence immunoassay with different strategies

For the fluorescence immunoassay of biomarkers, various strategies have been developed in the previous publications. Utilizing CdSe/ZnS quantum dot (QD) labeled antibodies as fluorescence signal material, a special fluorescence detection system for human serum albumin (HSA) detection has been developed. The system could detect fluorescence and convert it to photocurrent, the detection limit is approximately 32 ng mL^{-1}. [S3] An improved magnetic beads (MBs)-based fluorescence immunoassay method has been established by gold nanoparticles caused the fluorescence quenching of fluorescence in isothiocyanate. The detection limit for α-fetoprotein (AFP) assay is 8.5 ng mL^{-1}. [S4] Another fluorescence quenching

immunoassay method based on fluorescence quenching effects of gold nanoparticles for fluorescence in for human IgG detection has also been established. The fluorescence intensity of fluorescence is inversely proportional to the logarithm of the concentration of human IgG with a detection limit of 4.7 ng mL^{-1}.[S5] Furthermore, by combining the superior signal brightness and high photostability of quantum dots, a portable fluorescence biosensor for protein biomarker has been developed. Under optimal conditions, this sensor displays rapid responses for nitrated ceruloplasmin with a detection limit of 1.0 ng mL^{-1}. [S6] A more facile magnetic beads (MBs)-based time-resolved fluoroimmunoassay method has been successfully established and applied to the determination of tumor markers in human serum. Europium chelates are used to label antibody and generate a fluorescence and the detection limit is obtained to be 0.5 ng mL^{-1} for carcinoembryonic antigen (CEA) assay. [S7] Utilizing tyrosinase catalyzing the fluorescence quenching of dopamine (DA)-functionalized CdSe/ZnS quantum dots (QDs), a novel fluorescence quenching immunoassay method has also been established, and the detection limit is same to the above method. [S8] To explore more sensitive fluorescence immunoassay method, single wavelength excitation fluorescence cross-correlation spectroscopy is applied to the immunoassay of AFP. Fluorescent CdSe/ZnS quantum dots and the fluorophore Alexa Fluor 488 are used to label the antibodies. With these techniques, the limit of detection is reduced to 0.14 ng mL^{-1}. [S9] By utilizing amino-modified Mn-doped ZnS quantum dots (QDs) as solid supports, a direct fluorescent immunoassay is developed based on a fluorescent molecularly imprinted polymer (MIP), which is generated fluorescent turn-on by recognition with tumor biomarker. Thus, this detection method could allow the detection limit of CEA down to 0.04 ng mL^{-1}. The detection limits resulting from our method for AFP and C-reactive protein (CRP) are found to be 70 pg mL^{-1} and 30 pg mL^{-1}, respectively. Therefore, compared to these reported fluorescent immunoassay methods, our method shows higher sensitivity and lower fluorescence background.

Table S1. Comparison of fluorescence immunoassay for protein biomarkers with different Fluorescence labeled materials

Fluorescence labelled materials	Target analytes	Liner range ($ng \cdot mL^{-1}$)	LOD ($ng \cdot mL^{-1}$)	Ref.
CdSe/ZnS quantum dot	HSA	200-2.0×10^5	32	[S3]
fluorescein isothiocyanate	AFP	15-400	8.5	[S4]
fluorescein	human IgG	10-5000	4.7	[S5]
quantum dots	Nitrated ceruloplasmin	1-10000	1.0	[S6]
Europium chelates	CEA	1.0-1000	0.5	[S7]
CdSe / ZnS quantum dots	AFP	0.5-500	0.5	[S8]
CdSe/ZnS quantum dots	AFP	1.4-250	0.14	[S9]
Amino-modified Mn-doped ZnS quantum dots	AFB_1	0.05-10	0.048	[S10]
Without labels	CEA	0.1-100	0.04	[S11]
This work	AFP (CRP)	0.1-10	0.07 (0.03)	

9. The ^{1}H NMR, ^{13}C NMR and MS characterization of target compounds and intermediates

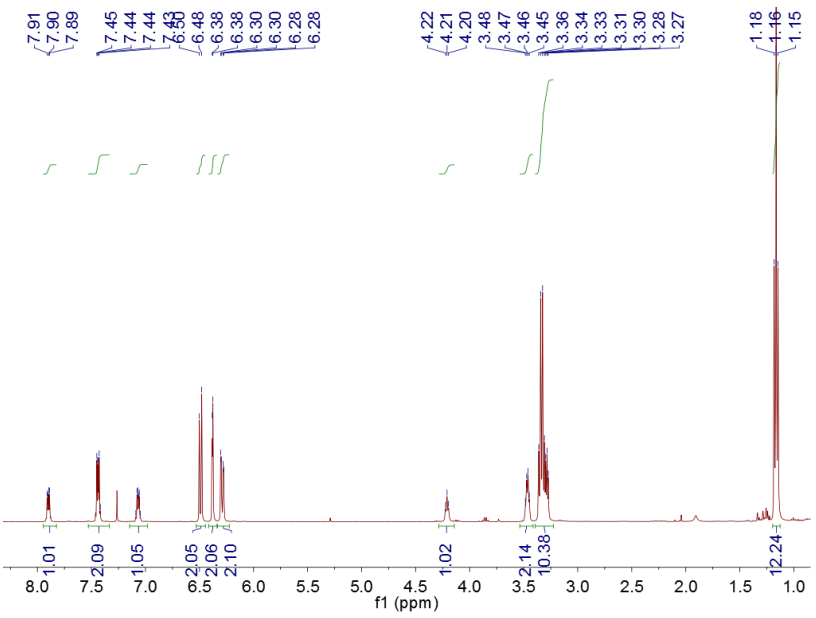

Figure S9. ^{1}H NMR spectrum of compound 1.

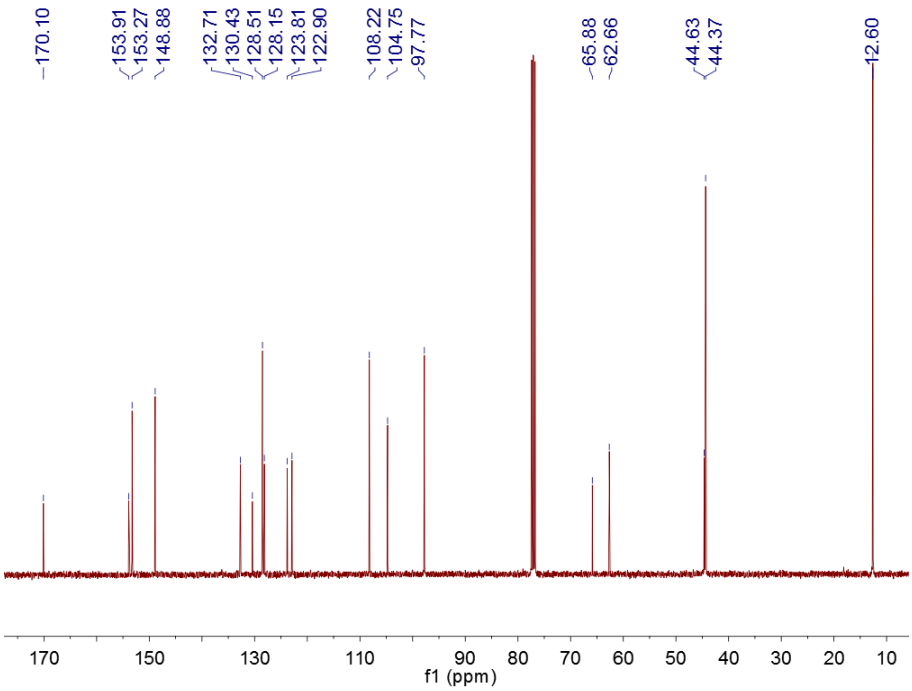

Figure S10. ^{13}C NMR spectrum of compound 1.

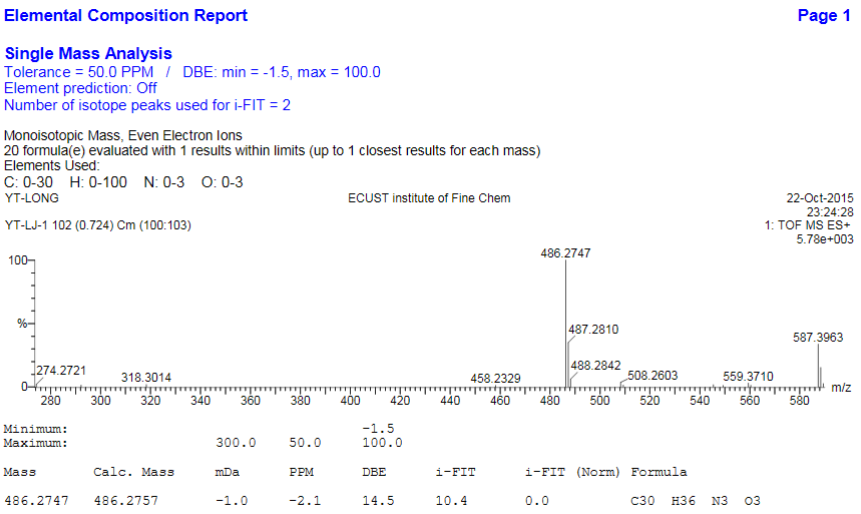

Figure S11. Mass spectrum of compound 1.

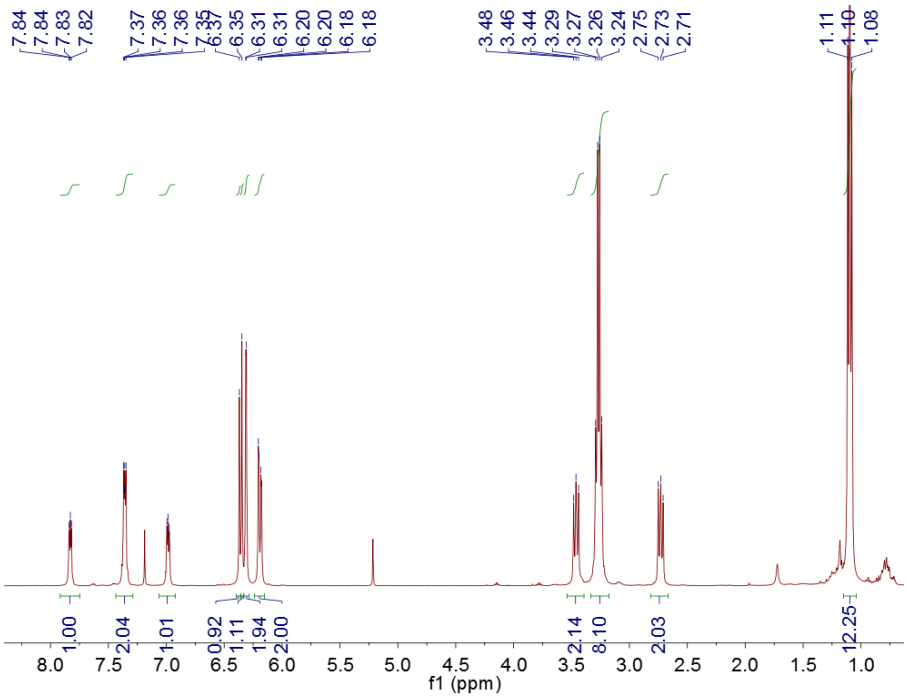

Figure S12. ^{1}H NMR spectrum of probe.

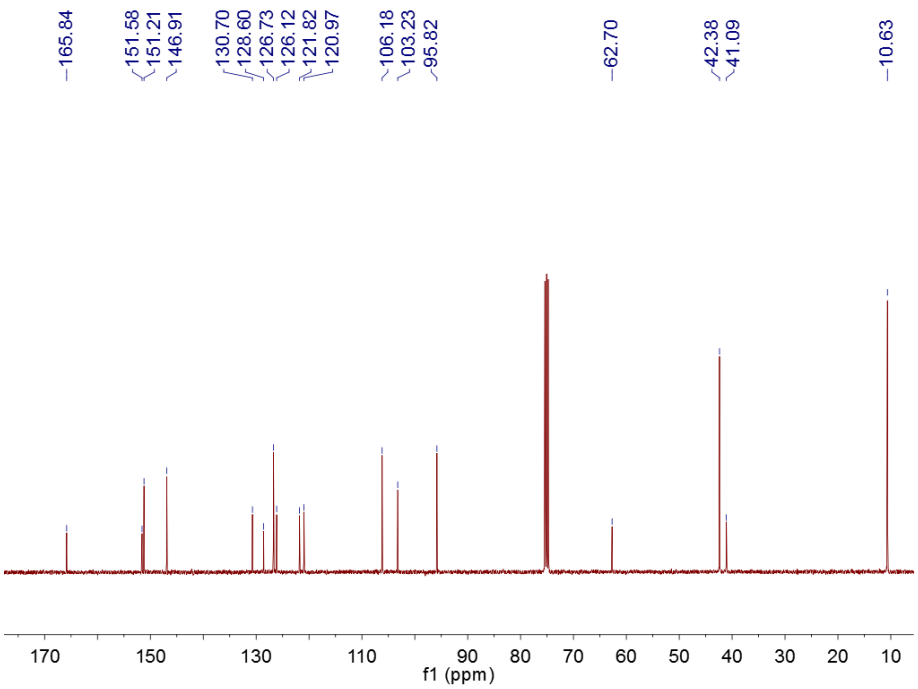

Figure S13. ^{13}C NMR spectrum of probe.

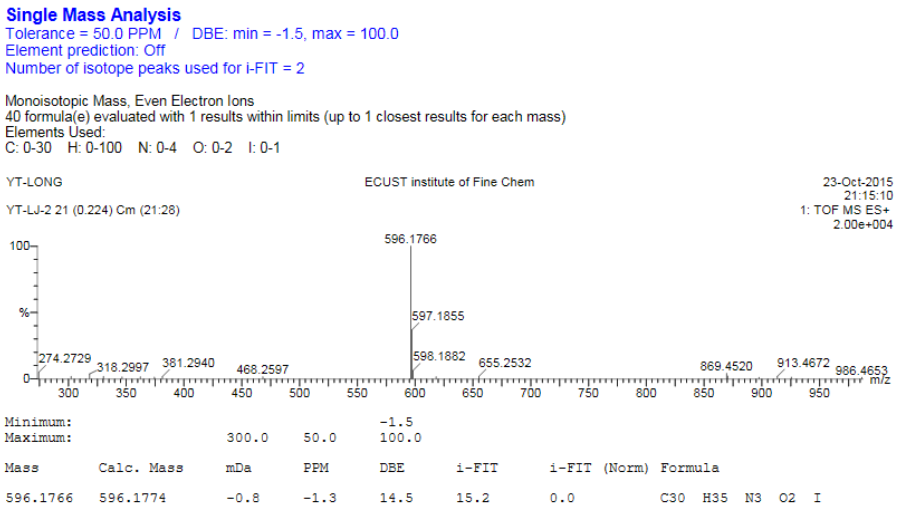

Figure S14. Mass spectrum of probe.

10. References

[S1] Tung NH, Chikae M, Ukita Y, Viet PH, Takamura Y. Sensing technique of silver nanoparticles as labels for immunoassay using liquid electrode plasma atomic emission spectrometry. Anal Chem. 2012; 84:1210-1213.

[S2] Yu RJ, Ma Wei, Liu XY, Jin HY, Han HX, Wang HY, Tian H, Long YT. Metal-linked immunosorbent assay (MeLISA): the enzyme-free alternative to ELISA for biomarker detection in serum. Theranostics. 2016; 6:1732-1739.

[S3] Tu MC, Changa YT, Kang YT, Chang HY, Chang P, Yew TR. A quantum dot-based optical immunosensor for human serum albumin detection. Biosens Bioelectron. 2012; 34:286-290.

[S4] Ao LM, Gao F, Pan BF, He R, Cui DX. Fluoroimmunoassay for antigen based on fluorescence quenching signal of gold nanoparticles. Anal Chem. 2006; 78:1104-1106.

[S5] Peng ZF, Chen ZP, Jiang JH, Zhang XB, Shen GL, Yu RQ. A novel immunoassay based on the dissociation of immunocomplex and fluorescence quenching by gold nanoparticles. Anal Chim Acta. 2007; 583:40-44.

[S6] Li ZH, Wang Y, Wang J, Tang ZW, Pounds JG, Lin YH. Rapid and sensitive detection of protein biomarker using a portable fluorescence biosensor based on quantum dots and a lateral flow test strip, Anal Chem. 2010; 82:7008-7014.

[S7] Hou JY, Liu TC, Lin GF, Li ZX, Zou LP, Li M, Wu YS. Development of an immunomagnetic bead-based time-resolved fluorescence immunoassay for rapid determination of levels of carcinoembryonic antigen in human serum. Anal Chim Acta. 2012; 734:93-98.

[S8] Zhang WH, Ma W, Long YT. Redox-Mediated Indirect Fluorescence Immunoassay for the Detection of Disease Biomarkers Using Dopamine-Functionalized Quantum Dots. Anal Chem. 2016; 88:5131-5136.

[S9] Wang JJ, Liu H, Huang XY, Ren JC. Homogeneous immunoassay for the cancer marker alpha-fetoprotein using single

wavelength excitation fluorescence cross-correlation spectroscopy and CdSe/ZnS quantum dots and fluorescent dyes as labels. Microchim Acta. 2016; 183:749-755.

[S10] Tan L, Chen K, Huang C, Peng RF, Luo XY, Yang R, Cheng YF, Tang YW. A fluorescent turn-on detection scheme for α-fetoprotein using quantum dots placed in a boronate-modified molecularly imprinted polymer with high affinity for glycoproteins. Microchim Acta. 2015; 182:2615-2622.

[S11] Yan M, Ge SG, Gao WQ, Chu CC, Yu JH, Song XR. Fluorescence immunosensor based on p-acid-encapsulated silica nanoparticles for tumor marker detection. Analyst. 2012; 137:2834-2839.